JOC Article

Experimental and Theoretical Studies of the Dimerizations of Imidoylketenes

Chun Zhou and David M. Birney*

Department of Chemistry and Biochemistry, Texas Tech University, Lubbock, Texas 79401-1061

david.birney@ttu.edu

Received July 31, 2003

Reaction conditions are presented that, for the first time, allow the generation and dimerization of *N*-alkylimidoylketenes, e.g. ,**1d**, while avoiding the intramolecular rearrangements observed under conventional conditions. The dimer of **1d** (**22a**) is the result of [4 + 2] cycloaddition across the C═C bond of one ketene. In contrast, the N−H imidoylketene **1c** dimerizes across the C═O bond to form **24b**. Furthermore, *N*-methylbenzoimidoylketene (**5b**), in equilibrium with the more stable benzoazetidinone **14b**, gives the formal [4 + 4] dimer **8b**. B3LYP/6-31G(d) transition structure calculations on these three modes of dimerization reproduce and offer explanations for these divergent regiochemistries. Both [4 + 2] dimerizations have planar, pseudopericyclic transition structures (**25a** and **29b**). Five transition structures were found for the formation of **8b**. A unique pseudopericyclic dimerization of **5b** with an orthogonal [4 + 4] geometry (**31**) has a barrier of only 0.7 kcal/mol. However, the overall lowest energy pathway involves concerted addition of **5b** across a σ bond in **14b** via **35**.

Introduction

Conjugated ketenes present a dense array of functionality and thus participate in a remarkable diversity of reactions.[1−6] Vinylketenes[2] and oxoketenes[3] have been widely used in synthesis and have been the focus of numerous mechanistic and computational studies as well. With a ketene, a C═N double bond, a nitrogen lone pair, and a possibly a substituent on nitrogen, imidoylketenes (sometimes called iminoketenes) potentially have an even richer chemistry. It is, however, the least developed. While there have been some computational studies,[2h,4] there have been relatively few experimental studies on imidoylketenes[3j,5] (**1**) or benzoimidoylketenes[6] (**5**). It has been difficult to generate and trap them while avoiding intramolecular reactions.[3j,5a,e,i−k] However, the obvious potential of these intermediates has encouraged our group and others to pursue this chemistry.[3j,5,6]

We now report the development of reaction conditions that, for the first time, allow us to generate a variety of substituted imidoylketenes (**1**) and benzoimidoylketenes (**5**) and observe bimolecular reactions. We confirm three different modes of dimerization of **1** and **5**, including two regioisomeric [4 + 2] pathways for **1** analogous to those found for oxoketenes[3a] and a novel [4 + 4] pathway for **5** (Scheme 1). We also report density functional theory calculations (B3LYP/6-31G(d)) that offer an explanation of these diverse dimerization pathways. We note that **6** is shown in Scheme 1 in analogy to **2** but is not observed, and not considered further, as it would involve loss of one aromatic ring.

(1) For reviews of conjugated ketenes, see: (a) Ulrich, H. In *Cycloaddition Reactions of Heterocumulenes*; Blomquist, A. T., Ed.; Academic Press: New York, 1967; Vol. 9, pp 38−109. (b) Moore, H. W.; Decker, O. H. W. *Chem. Rev.* **1986**, *86*, 821−830. (c) Hyatt, J. A.; Raynolds, P. W. In *Organic Reactions*; Paquette, L. A., Ed.; John Wiley & Sons: New York, 1994; Vol. 45, pp159−636. (d) Wentrup, C.; Heilmayer, W.; Kollenz, G. *Synthesis* **1994**, 1219−1248. (e) Tidwell, T. T. *Ketenes*; John Wiley & Sons: New York, 1995.

(2) For leading references, see refs 1 and: (a) Barton, D. H. R.; Chung, S. K.; Kwon, T. W. *Tetrahedron Lett.* **1996**, *37*, 3631−334. (b) Niwayama, S.; Kallel, E. A.; Sheu, C.; Houk, K. N. *J. Org. Chem.* **1996**, *61*, 2517−2522. (c) Collomb, D.; Doutheau, A. *Tetrahedron Lett.* **1997**, *38*, 1397−1398. (d) Bibas, H.; Koch, R.; Wentrup, C. *J. Org. Chem.* **1998**, *63*, 2619−2626. (e) Mingo, P.; Zhang, S.; Liebeskind, L. *J. Org. Chem.* **1999**, *64*, 2145−2146. (f) Bennett, D. M.; Okamoto, I.; Danheiser, R. L. *Org. Lett* **1999**, *1*, 641−644. (g) Sharma, A. K.; Kumar, R. S.; Mahajan, M. P. *Heterocycles* **2000**, *52*, 603−619. (h) Zhou, C.; Birney, D. M. *J. Am. Chem. Soc.* **2002**, *124*, 5231−5241.

(3) For leading references, see refs 1, 2h, and: (a) Kappe, C. O.; Farber, G.; Wentrup, C.; Kollenz, G. *J. Org. Chem.* **1992**, *57*, 7078−7083. (b) Gammill, R. B.; Judge, T. M.; Phillips, G.; Zhang, Q.; Sowell, C. G.; Cheney, B. V.; Mizsak, S. A.; Dolak, L. A.; Seest, E. P. *J. Am. Chem. Soc.* **1994**, *116*, 12113−12114. (c) Liu, R. C.-Y.; Lusztyk, J.; McAllister, M. A.; Tidwell, T. T.; Wagner, B. D. *J. Am. Chem. Soc.* **1998**, *120*, 6247−6251. (d) Brown, D. G.; Hoye, T. R.; Brisbois, R. G. *J. Org. Chem.* **1998**, *63*, 1630−1636. (e) Sato, M.; Iwamoto, K. *J. Synth. Org. Chem., Jpn.* **1999**, *57*, 76−83. (f) Nguyen, M. T.; Landuyt, L.; Nguyen, H. M. T. *J. Org. Chem.* **1999**, *64*, 401−407. (g) Cevasco, G.; Vigo, D.; Thea, S. *Org. Lett.* **1999**, *1*, 1165−1167. (h) Murata, S.; Kobayashi, J.; Kongou, C.; Miyata, M.; Masushita, T.; Tomioka, H. *J. Org. Chem.* **2000**, *65*, 6082−6092. (i) Ammann, J. R.; Flammang, R.; Wong, M. W.; Wentrup, C. *J. Org. Chem.* **2000**, *65*, 2706−2710. (j) Shumway, W. W. *Diastereoselectivity and Reactivity of Oxoketene and Imidoylketene: Investigating the Pseudopericyclic Reaction Mechanism*; Texas Tech University: Lubbock, TX, 2001. (k) Emtenäs, H.; Alderin, L.; Almqvist, F. *J. Org. Chem.* **2001**, *66*, 6756−6761. (l) Lucas, N. C. d.; Netto-Ferreira, J. C.; Andraos, J.; Scaiano, J. C. *J. Org. Chem.* **2001**, *66*, 5016−5021. (m) Stadler, A.; Zangger, K.; Belaj, F.; Kollenz, G. *Tetrahedron* **2001**, *57*, 6757−6763. (n) Shumway, W. W.; Dalley, N. K.; Birney, D. M. *J. Org. Chem.* **2001**, *66*, 5832−5839. (o) Saripinar, E.; Ilhan, I. O.; Akcamur, Y. *Heterocycles* **2002**, *57*, 1445−1459. (p) Wallfisch, B. C.; Belaj, F.; Wentrup, C.; Kappe, C. O.; Kollenz, G. *J. Chem. Soc., Perkin Trans. 1* **2002**, 599−605.

(4) (a) Nguyen, M. T.; Ha, T.; More O'Ferrall, R. A. *J. Org. Chem.* **1990**, *55*, 3251−3256. (b)Eisenberg, S. W. E.; Kurth, M. J.; Fink, W. H. *J. Org. Chem.* **1995**, *60*, 3736−3742. (c) Ham, S.; Birney, D. M. *J. Org. Chem.* **1996**, *61*, 3962−3968.

10.1021/jo035128o CCC: $27.50
Published on Web 12/09/2003

SCHEME 1

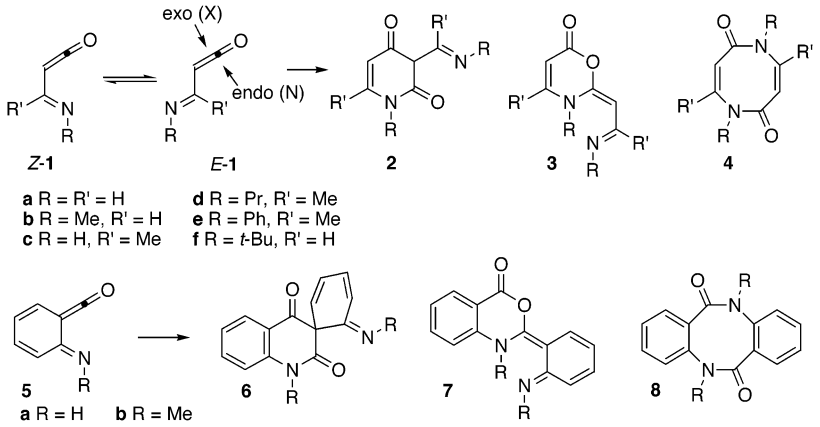

The first challenge in the study of imidoylketenes is the development of methods for their generation. In this work, we evaluate the methods by the formation of dimers. In subsequent work, we will report on trapping with other reagents. Given the close structural analogy between imidoylketenes and oxoketenes, a comparison of reactions that generate oxoketene is instructive. While pyrolysis of β-ketoesters cleanly generates oxoketenes,[1d,5j] the only observed products from pyrolysis of *N*-alkylenaminoesters (e.g., **9a**) are enaminoaldehydes (**11**) (eq 1).[3j,5a,n,o] The latter are formed via a 1, 5-hydrogen shift in the imidoylketene[5n,o] (e.g., **1d**) to form **10** and tautomerization. Attempts to generate *N*-phenylimidoylketenes (e.g., **1e**) are similarly thwarted by an intramolecular cyclization reaction forming **12** (eq 2).[5a,g,j,k,n] Although α-diazoketones are useful precursors for ketenes, α-diazoimines are not because they spontaneously undergo a pseudopericyclic 1,5-electrocyclization.[5e,h−j,7]

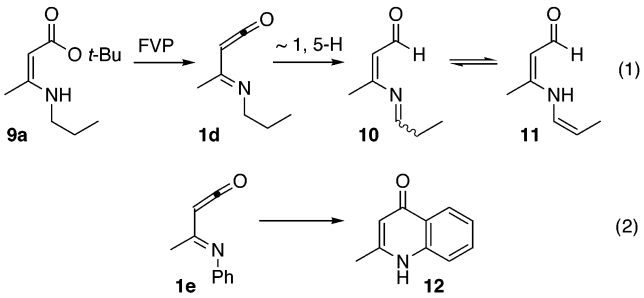

The few reported examples of imidoylketenes tend to have an unreactive group on the imino nitrogen.[2d,5,6] Suschitzky et al. found that heating either **13a** with loss of CO_2 or **16** with loss of nitrogen gave the benzoxazinone (**15a**)[6b] (eq 3). The product was considered to arise by dimerization of the benzoimidoylketene intermediate **5a** through a Diels−Alder reaction. Presumably, **5a** is in equilibrium with its more stable valence isomer, benzoazetinone **14a**.[6d,e,f] Maujean et al.[5a] obtained the dimerization products **17a** and **17b** from **1f** by [4 + 2] cycloaddition across the C=C double bond (eq 4) when they pyrolyzed the ethyl *N*-*tert*-butyl enamino ester **9b** at 450 °C and 15 Torr. Wentrup has reported the reversible dimerization of a number of (2-pyridyl)-ketenes.[2d,5k−m]

In addition, dianthranilide **8b** was isolated from thermolysis of **18** (Scheme 2).[8] The authors postulated a

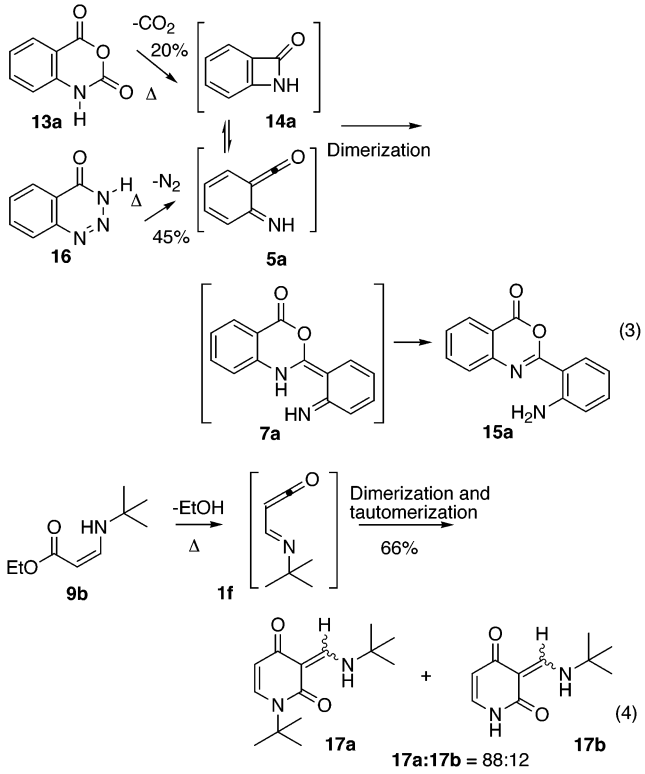

stepwise mechanism in which a molecule of **19** reacts with a molecule of a highly electrophilic benzoazetinone **14b**, which is itself formed from **18**, to give the dimeric monoamide (**20**). Compound **20** was then proposed to cyclize to **8b** with the expulsion of MeOH.

SCHEME 2

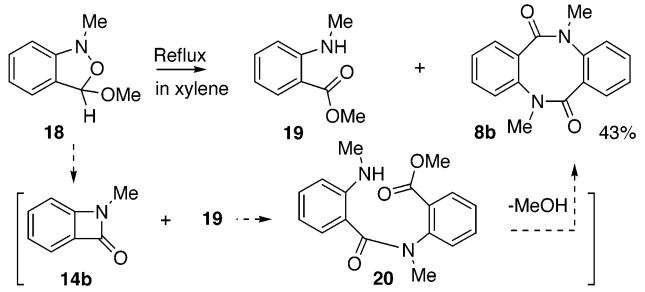

Since compound **8b** structurally is a dimer of the benzoimidoylketene **5b**, one might ask whether it might be formed directly from the equilibrium mixture of **14b**[6e,f] and **5b**, without the intervention of an external nucleophile. If so, which participates in the dimerization, **14b** or **5b**? And what is the origin of the dramatic chemoselectivity, whereby **14a** gives **15a** via an overall [4 + 2] cycloaddition while **14b** gives **8b** via an overall [4 + 4]? If compound **8b** is indeed formed via a [4 + 4] cycloaddition,[6f] this demands an explanation, since such reactions of hydrocarbons are orbital symmetry forbidden and concerted examples are not known.[9]

In addition, there is a significant difference in chemoselectivity in the [4 + 2] cycloadditions. The two-atom component can react either across the C═C bond, as in **17a**, or across the C═O bond as in **15a**. What are the origins of this chemoselectivity? How general is it? This work seeks to answer of these questions as well.

Results and Discussion

As discussed above, the pyrolysis of enaminoesters (**9**) would appear to be a convenient method to generate imidoylketenes, as these are readily obtained from β-keto esters and primary amines. Indeed, we had previously shown that heating a solution of **9a** in the presence of another alcohol led to transesterification, presumably via the imidoylketene **1d**.[5j] However, we were unable to obtain adducts of **1d** with less reactive traps (nor did we observe dimerization) presumably because of reversible trapping with the *tert*-butyl alcohol byproduct. Furthermore, the thermal unimolecular reaction of N-substituted imidoylketenes under FVP conditions has restricted this to tertiary substituents, e.g., **1f**[5a] or unsubstituted derivatives (e.g., **5a**[6]). After exploring a number of reaction conditions, we found that heating **9a** at 150 °C, under N_2, where the *tert*-butyl alcohol byproduct was distilled off, could prevent the back-reaction. In the absence of other trapping reagents, two products were obtained, **21a** and **22a** (Scheme 3). The former appears to be formed by the [4 + 2] cycloaddition of **1d** with **9a**, followed by loss of propylamine. Significantly, no products from rearrangement of **1d** are observed under these conditions. Interestingly, the dimer **22a** (from tautomerization of **2d**) is formed by trapping of the ketene C═C double bond, in analogy to dimerization of most α-oxoketenes[1,3n] and of the N-*tert*-butyl derivative **1f**,[5a] but in contrast to the unsubstituted derivative **1c** (below). Preliminary results indicate that **1d** can be reacted with a number of reagents under these conditions. These will be reported in due course.

SCHEME 3

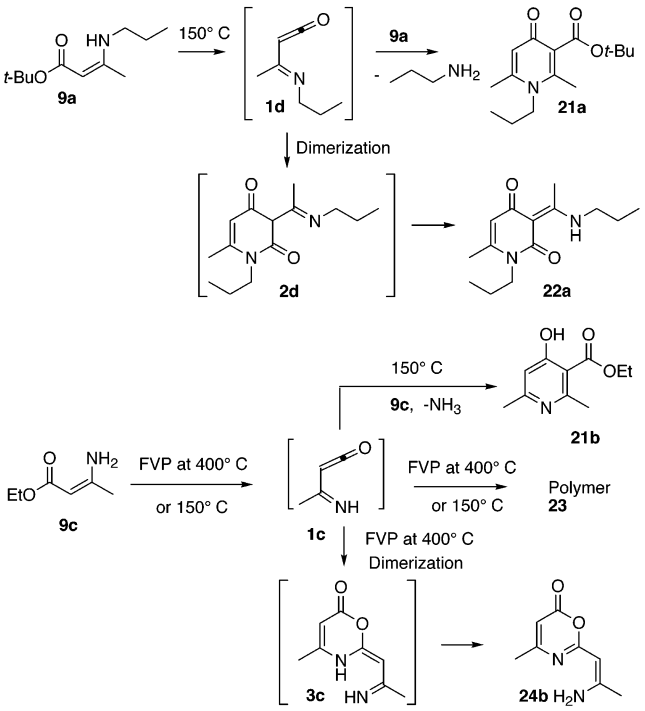

We reasoned that an imidoylketene lacking a substituent on the nitrogen would be unable to undergo intramolecular reactions and might be more readily trapped. Indeed, when **9c** was subjected to FVP at 400 °C under approximately 0.25 Torr vacuum, the products were consistent with the formation of **1c** (Scheme 3). There was a substantial amount of polymeric material (**23**), elemental analysis of which suggested it was a polymer of **1c**,[10] with some replacement of NH by O, as expected for hydrolysis of enamines. In addition, a small amount of the dimer **24b** was also obtained. Interestingly, this has the same regiochemistry as dimerization of **5a** (but not as **1f** or **1d**) with trapping across the C═O bond of **1c** and subsequent tautomerization of **3c** to **24b**. Steric crowding in oxoketenes can lead to this regiochemistry,[3a,m,p] but a different cause must be operative here

(5) (a) Maujean, A.; Marcy, G.; Chuche, J. *Thetrahedron Lett.* **1980**, 519−522. (b) Cheikh, A. B.; Chuche, J.; Manisse, N.; Pommelet, J. C.; Netsch, K.-P.; Lorencak, P.; Wentrup, C. *J. Org. Chem.* **1991**, *56*, 970−975. (c) Kappe, C. O.; Kollenz, G.; Leung-Toung, R.; Wentrup, C. *J. Chem. Soc., Chem. Commun.* **1992**, 487−488. (d) Kappe, C. O.; Kollenz, G.; Netsch, K.-P.; Leung-Toung, R.; Wentrup, C. *J. Chem. Soc., Chem. Commun.* **1992**, 488−490. (e) Clarke, D.; Mares, R. W.; McNab, H. *J. Chem. Soc., Chem. Commun.* **1993**, 1026−1027. (f) Aliev, Z. G.; Maslivets, A. N.; Krasnykh, O. P.; Andreichikov, Y. S.; Atovmyan, L. O. *Russ. Chem. Bull.* **1993**, *42*, 1569−1572. (g) Chuburu, F.; Lacombe, S.; Gullouzo, G. P.; Wentrup, C. *New J. Chem.* **1994**, *18*, 879−888. (h) Fulloon, B.; El-Nabi, H. A. A.; Kollenz, G.; Wentrup, C. *Tetrahedron Lett.* **1995**, *36*, 6547−6550. (i) Fulloon, B. E.; Wentrup, C. *J. Org. Chem.* **1996**, *61*, 1363−1368. (j) Birney, D. M.; Xu, X.; Ham, S.; Huang, X. *J. Org. Chem.* **1997**, *62*, 7114−7120. (k) Rao, V. V. R.; Fulloon, B. E.; Bernhardt, P. V.; Koch, R.; Wentrup, C. *J. Org. Chem.* **1998**, *63*, 5779−5786. (l) Plüg, C.; Kuhn, A.; Wentrup, C. *J. Chem. Soc., Perkin Trans. 1* **2002**, 1366−1368. (m) Andersen, H. G.; Bednarek, P.; Wentrup, C. *J. Phys. Org. Chem.* **2003**, *16*, 519−524. (n) Briehl, H.; Lukosch, A.; Wentrup, C. *J. Org. Chem.* **1984**, *49*, 2772−2779. (o) Gordon, H. J.; Martin, J. C.; McNab, H. *J. Chem. Soc., Perkin Trans. 1* **1984**, 2129−2132. (p) Netsch, K.-P. Ph.D. Thesis, University of Marburg, Marburg, 1985.

(6) (a) Herlinger, H. *Angew. Chem., Int. Ed. Engl.* **1964**, *3*, 378.(b) Smalley, R. K.; Suschitzky, H.; Tanner, E. M. *Tetrahedron Lett.* **1966**, 3465−369. (c) Crabtree, H. E.; Smalley, R. K.; Suschitzky, H. *J. Chem. Soc. C* **1968**, 2730−2733. (d) Chiu, S.; Chou, C. *Tetrahedron Lett.* **1999**, *40*, 9271−9272. (e) Wentrup, C.; Gross, G. *Angew. Chem., Int. Ed. Engl.* **1983**, *22*, 543. (f) Wentrup, C.; Bender, H.; Gross, G. *J. Org. Chem.* **1987**, *52*, 3838−3847.

(7) Huisgen, R. *Angew. Chem., Int. Ed. Engl.* **1980**, *19*, 947−973.

(8) Vander Meer, R. K.; Olofson, R. A. *J. Org. Chem.* **1984**, *49*, 3373−3377.

(9) (a) Miller, B. *Advanced Organic Chemistry*, 2nd ed.; Prentice Hall: Upper Saddle River, 2004. (b) Dimerization of orthoxylene gives some 1,5-dibenzocyclooctadiene via what appears to be a biradical pathway. Errede, L. A. *J. Am. Chem. Soc.* **1961**, *83*, 949−954. (c) Woodward, R. B.; Hoffmann, R. *The Conservation of Orbital Symmetry*; Verlag Chemie, GmbH: Weinheim, 1970.

(10) Polymeric material is obtained from oxoketenes as well. (a) Nikolaev, V. A.; Korneef, S. M.; Terent'eva, I. V.; Korobitsyna, I. K. *J. Org. Chem. USSR, Engl. Trans.* **1991**, *27*, 1845. (b) Freiermuth, B.; Wentrup, C. *J. Org. Chem.* **1991**, *56*, 2286−2289.

SCHEME 4

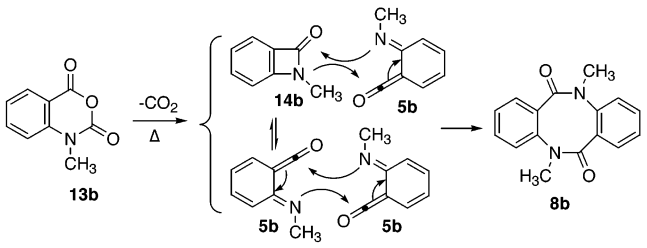

and will be addressed below. A similar regiochemistry has been reported for the dimerization of another NH-imidoylketene.[5p]

When we submitted **9c** to reaction conditions similar to those for **9a** above, a significant amount of polymer **23** was obtained (Scheme 3). No **24b** was found, but a very small amount of **21b** was also isolated. This product is analogous to **21a**, but is the phenolic tautomer. It seems that the unsubstituted imidoylketene **1c** is particularly prone to polymerization.

On the basis of the observed regiochemical preference in the dimerization, it appears that the presence of an imino NH is needed for obtaining the regiochemistry observed in dimers **15a** and **24b**. We reasoned that a substituted benzoimidoylketene might lead to different chemistry as compared to **5a**. Indeed, we found that refluxing **13b** in mesitylene with slow liberation of CO_2 gave the eight-membered ring product **8b** instead of any six-membered dimerization product (Scheme 4). Obviously, **8b** could not be explained to form by using the mechanism Olofson et al. proposed[8] for the reaction of **18** (Scheme 2) since there is no external nucleophile and no compound analogous to **19** can be formed. Instead, formation of **8b** can only occur from the reaction of **5b** and **14b**.

These results raise several questions that we sought to answer computationally. What are the factors that influence the regiochemistry of dimerization of imidoylketenes? What is the role of the imino NH? Are the [4 + 2] dimerizations stepwise or concerted? And if concerted, are they pericyclic as Suschitzky et al. proposed[6b] or pseudopericyclic as our computational and experimental results indicate for the dimerization of α-oxoketenes?[3n] Is the apparent [4 + 4] dimerization to form **8b** a concerted, pseudopericyclic process, or does it follow a stepwise pathway?

Computational Methods. All calculations were carried out using Gaussian 98[11] with the B3LYP[12a] hybrid functional using 6-31G(d) basis set.[12b] Frequency calculations verified the identity of each stationary point as a minimum or a transition structure. In some cases, intrinsic reaction coordinate (IRC) calculations[13] were performed to connect the transition structures to their respective minima. In other cases, the motion of the imaginary frequency unambiguously showed the reactants and products. For some selected transition structure structures, natural bond orbital (NBO) analyses[14] were performed. Zero-point vibrational energy (ZPE) corrections have been applied, but not scaled.

TABLE 1. Calculated Relative Energies with Zero-Point Vibrational Energy (ZPE) Corrections (kcal/mol) and Low or Imaginary Frequencies (cm^{-1}) at the B3LYP/6-31G(d) Level Relative to Figure 1; Dimerization of 1a

structure	relative energy[a] + ZPE	low frequency
2a	−44.2	58.1
3a	−46.8	88.0
4a	−43.1	51.0
24a	−56.3	79.4
25a	3.7	104.0i
26	−46.4	1330.8i
27a	2.5	153.2i
28a	4.7	178.3i
29a	5.7	173.5i
30	7.2	84.3i

[a] Energies are relative to the most stable complex (3.5 kcal/mol more stable than two molecules of **1a**, see Table S1 (Supporting Information)).

A comprehensive computational study requires locating all possible conformational isomers of the ground and transition structures. For the parent imidoylketene **1a**, there are four calculated conformational minima, *Z* and *E* around the imine double bond and *s*-*Z* and *s*-*E* around the single bond.[2h,4c] (See Figure S3 (Supporting Information) for conformations of **1b**.) We have previously shown that the more reactive conformers are the two *E*-imines.[2h,4c] Such conformers are seen in argon matrixes.[5m] In light of this, and for simplicity and clarity, we consider only the single-bond conformers and refer to them as *E*-**1a** and *Z*-**1a** (Scheme 1). In the [4 + 2] dimerization, we assume that the 4-atom component is *Z*-**1a**. The 2-atom component can be either *E* or *Z* and can be attacked either exo or endo as in Scheme 1. Since there are two regioisomeric products, **2a** and **3a** (the latter giving **24b**), there are a total of eight possible pathways. These were explored in detail for the dimerization of both **1a** and **1b** because unsubstituted and substituted imidoylketenes show different regioselectivity. In addition, transition structures were located for product interconversions, for the ring openings of **14** to **5** and the [4 + 4] cycloadditions of **1a**, **1b**, and **5b**. This gives a total of 33 structures related to **1a**, 32 for **1b**, and 19 for **5b**. In view of this large number of structures, only important and representative transition structures are shown in Figures 1−3 with relative energies and low frequencies in Tables 1−3. Side and top views, more detailed geometries, energies, low-frequency vibrations, and ZPE corrections of all reactants, complexes, transition structures, and products are shown in the Supporting Information (Figures S1−S6 and Tables S1−S3).

(11) Frisch, M. J.; Trucks, G. W.; Schlegel, H. B.; Scuseria, G. E.; Robb, M. A.; Cheeseman, J. R.; Zakrzewski, V. G.; Montgomery, Jr., J. A.; Stratmann, R. E.; Burant, J. C.; Dapprich, S.; Millam, M. J.; Daniels, A. D.; Kudin, K. N.; Strain, M. C.; Farkas, O. Tomasi, J.; Barone, V.; Cossi, M.; R. Cammi, B. Mennucci, C. Pomelli, C. Adamo, S. Clifford, J. Ochterski, G. A. Petersson, P. Y. Ayala, Q. Cui, K. Morokuma, D. K. Malick, A. D. Rabuck, K. Raghavachari, J. B. Foresman, J. Cioslowski, J. V. Ortiz, B. B. Stefanov, G. Liu, A. Liashenko, P. Piskorz, I. Komaromi, R. Gomperts, R. L. Martin, D. J. Fox, T. Keith, M. A. Al-Laham, C. Y. Peng, A. Nanayakkara, C. Gonzalez, M. Challacombe, P. M. W. Gill, B. Johnson, W. Chen, M. W. Wong, J. L. Andres, C. Gonzalez, M. Head-Gordon, E. S. Replogle, and J. A. Pople, *Gaussian 98*, Revision A.6; Gaussian, Inc., Pittsburgh, PA, 1998.

(12) (a) Becke, A. D. *J. Chem. Phys.* **1993**, *98*, 5648−5652. (b) Hariharan, P. C.; Pople, J. A. *Theor. Chim. Acta* **1973**, *28*, 213.

(13) (a) Fukui, K. *Acc. Chem. Res.* **1981**, *14*, 363−368. (b) Gonzalez, C.; Schlegel, H. B. *J. Phys. Chem.* **1990**, *94*, 5523.

(14) (a) Weinhold, F.; Carpenter, J. E. *The Structure of Small Molecules and Ions*, Plenum: New York, 1988. (b) Reed, A. E.; Curtiss, L. A.; Weinhold, F. *Chem. Rev.* **1988**, *88*, 899−926.

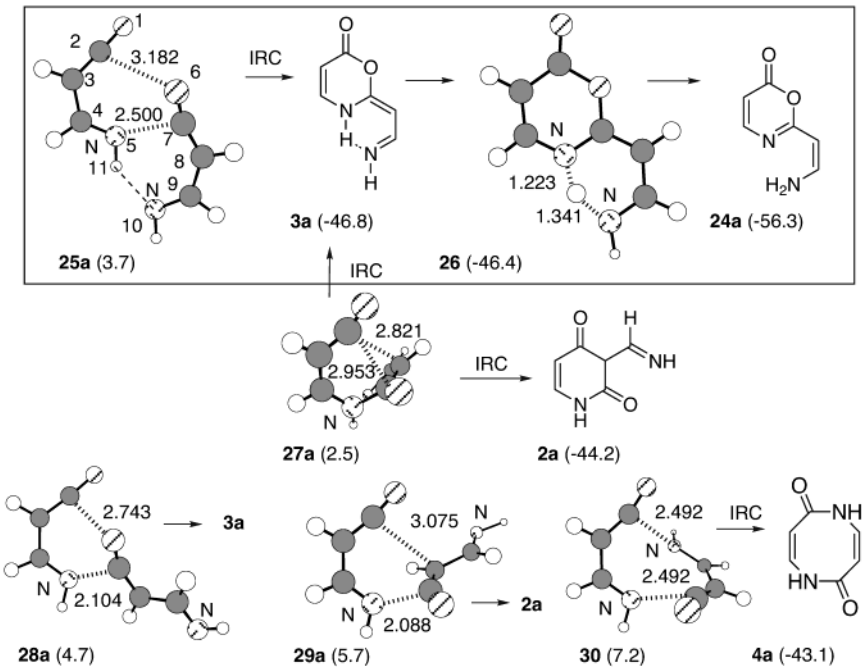

FIGURE 1. Selected B3LYP/6-31G(d)-optimized transition structures for dimerization reactions of **1a**. Distances are shown in angstroms. Carbons are shaded, hydrogens are open, oxygens are striped, and nitrogens are labeled. Close approaches and/or H-bonds are indicated as dashed lines and partial bonds as hash marks. Relative energies (kcal/mol) are in parentheses. The lowest energy pathway is boxed. IRC indicates the reaction coordinate was followed explicitly and connects the two indicated structures.

TABLE 2. Calculated Relative Energies with Zero-Point Vibrational Energy (ZPE) Corrections (kcal/mol) and Low or Imaginary Frequencies (cm^{-1}) at the B3LYP/6-31G(d) Level Related to Figure 2; Dimerization of 1b

structure	relative energy[a] + ZPE	low frequency
2b	−44.3	51.9
22b	−69.2	60.4
29b	3.9	136.7i

[a] Energies are relative to the most stable complex (2.1 kcal/mol more stable than two molecules of **1b**, see Table S2 (Supporting Information)).

TABLE 3. Calculated Relative Energies with Zero-Point Vibrational Energies (ZPE) Corrections (kcal/mol) and Low or Imaginary Frequencies (cm^{-1}) at the B3LYP/6-31G(d) Level Related to Figure 3; Dimerization of 14b and 5b

structure	relative energy[a] + ZPE	low frequency
14b		82.0
5b	13.0	79.6
8b	−64.3	46.3
31	26.7	74.8i
32	35.8	408.7i
33	32.8	280.7i
34	7.7	318.1i
35	19.6	177.9i

[a] Energies are relative to one or two molecules of **14b** as appropriate. See Table S3 (Supporting Information).

As reported for ketenes with other reagents,[2d,h,15] complexes between two imidoylketene monomers were found (Figures S1 and S3 (Supporting Information)). The most stable complex in each series is used as the zero of energy in the tables. The tautomeric equilibria between non-benzo-fused imidoylketenes and their corresponding azetinones have previously been calculated, and the imidoylketenes are more stable than their azetinones.[16] The stabilities of benzo-fused imidoylketenes **5a** and **5b** and their corresponding azetinones **14a** and **14b** were calculated in this work (Figure S5 and Table S3 (Supporting Information)).

Computational Results

Dimerization of Imidoylketene 1a. As described above, four pathways each to the two regioisomeric six-membered ring products were considered for the [4 + 2] dimerization of **1a**. The lowest energy pathway is shown in Figure 1, addition across the C═O bond to ultimately yield **24a**. Representative transition structures for the alternative [4 + 2] and [4 + 4] cycloadditions are also shown.

The lowest energy of the eight pathways for [4 + 2] dimerization is via the transition structure **25a**, which is only 3.7 kcal/mol above the lowest energy complex. IRC calculations confirm that this gives the product of addition across the C═O double bond, **3a**. The low barrier and approximate planarity of this transition structure are consistent with a pseudopericyclic transition structure.[2d,h,3n,4c,17] Although the *E*-geometry is more stable and exo attack less sterically crowded[2h,4c] (see below), the geometry clearly indicates that this one

(15) (a) Sung, K.; Tidwell, T. T. *J. Am. Chem. Soc.* **1998**, *120*, 3043−3048. (b) Couturier-Tamburelli, I.; Aycard, J. P.; Wong, M. W.; Wentrup, C. *J. Phy. Chem. A.* **2000**, *104*, 3466−3471. (c) Kuhn, A.; Plüg, C.; Wentrup, C. *J. Am. Chem. Soc.* **2000**, *122*, 1945−1948.

(16) (a) Pericas, M. A.; Serratosa, F.; Valenti, E.; Font-Altaba, M.; Solans, X. *J. Chem. Soc., Perkin Trans. 2*, **1986**, 961−967. (b) An azetinone has been observed. Kappe, C. O.; Kollenz, G.; Netsch, K.-P.; Leung-Toung, R.; Wentrup, C. *J. Chem. Soc., Chem. Commun.* **1992**, 488−490. See also Figure S5 and Table S3 (Supporting Information).

structure is uniquely stabilized by a hydrogen bond from N_5-H_{11} to N_{10}. The adduct **3a** then undergoes an almost barrierless proton transfer via a planar, pseudopericyclic transition structure **26** (0.4 kcal/mol above **3a**) to give the more stable (by 9.5 kcal/mol) tautomer **24a**. This pathway is in accord with our experimental result that pyrolysis of **9c** gives **24b** as the only isolated dimer, albeit in low yield.

We could not locate a transition structure for a direct [4 + 2] cycloaddition to give the regioisomer **2a** from addition across the ketene C=C bond of *Z*-**1a**. We did find **27a**; following the IRC from this structure leads to the two regioisomeric products, **3a** and **2a** (Figure 1, Table S2 (Supporting Information)). This is a forbidden 1,3-sigmatropic rearrangement and has a relatively high barrier of 46.7 kcal/mol above **2a**. Because transition structure **25a** leads to the same product (**3a**) and is higher in energy than **27a** (albeit by only 1.2 kcal/mol), we looked for a connection between the two transition structures on the potential energy surface. (See Figure S7-a and Tables S4 and S5 (Supporting Information).) No distinguishing connection such as a sequential transition structure or a valley-ridge inflection point was found.[18] Although there might be a downhill pathway from **25a** to **2a** via **27a**, the steepest descent is clearly toward **3a**, corresponding to the observed products in imidoylketenes lacking a substituent on the nitrogen.

For the [4 + 2] dimerization of *Z*-**1a** and *E*-**1a**, we could locate both regioisomeric transition structures (**28a** and **29a**); the lower energy pathway with this conformation involves sterically less crowded exo attack across the C=O bond (**28a**, 4.7 kcal/mol, Figure 1). In the current case, an exo [4 + 2] transition structure across C=C double bond was also located (**29a**, 5.7 kcal/mol). These [4 + 2] transition structures are higher in energy, presumably because they lack the hydrogen bond of **25a**.

A concerted [4 + 4] transition structure (**30**, 7.2 kcal/mol) was located. An IRC calculation confirmed that this leads to an eight-membered product, **4a**. Although suprafacial [4 + 4] cycloadditions of hydrocarbons are forbidden[9] and would not be expected to have such a low barrier, the orbital overlap is clearly not suprafacial. To the best of our knowledge, this is a unique transition structure; the two ketenes are almost orthogonal. Any π-overlap would be antarafacial−antarafacial which would also be forbidden. However, the geometry indicates that the imine lone pairs are attacking the ketene in-plane. This means the orbital overlap is pseudopericyclic and allowed, rather than of pericyclic and forbidden. This modest barrier (7.2 kcal/mol) is nevertheless larger than that for the [4 + 2] dimerization via **25a** (3.7 kcal/mol), perhaps in part reflecting the greater stability of the [4 + 2] product (**3a**, −46.8 kcal/mol vs **4a**, −43.1 kcal/mol). To our knowledge, no eight-membered rings have been reported for dimerization of NH-imidoylketenes, consistent with the higher calculated barrier. A 1,3-sigmatropic transition structure was located as well, connecting **4a** and **2a** (see Figure S2 (Supporting Information), structure *ZZ*-**37a**-N-TS).

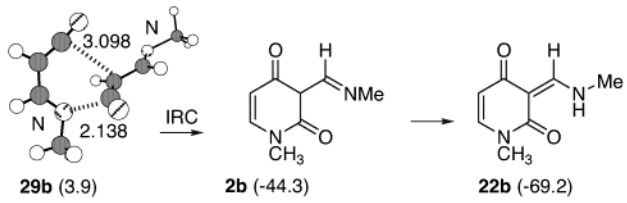

FIGURE 2. Lowest energy B3LYP/6-31G(d)-optimized transition structure for dimerization of **1b**. See Figure 1 for key.

Why do these [4 + 2] and [4 + 4] transition structures have relatively low energy calculated barriers as compared to the common Diels−Alder [4 + 2] cycloadditions? For the dimerization reactions between two molecules of *Z*-**1a**, the transition structure, **25a**, has an almost planar geometry and NBO analysis shows that it is the in-plane lone pair on the N_5 that donates electrons ($\Delta E_2 = 10.19$ kcal/mol) to antibonding π bond of C_7-O_6, forming the new bond C_7-N_5. The geometries of the transition structures for the dimerization of *Z*-**1a** and *E*-**1a**, although less planar, have similar orbital interactions. All these data show that for all the transition structures, there is at least one orbital disconnection during the concerted [4 + 2] cycloadditions to form the six membered ring products. Thus these reactions are pseudopericyclic reactions as our group[2h,3n,4c,17a−e] and others[2d,17f−k] found for related reactions, instead of classical D−A reaction as Suschitzky[6b] proposed.

Dimerization of *N*-Methylimidoylketene 1b. Experimentally, N-substituted imidoylketenes dimerize across the C=C bond, a regiochemistry different from the NH ones above. A methyl group was used as the simplest computational model for an alkyl substituted imidoylketene. The most stable complex between two molecules of **1b** (Figure S3, Table S2 (Supporting Information)) is used as the energy reference.

In this case, all eight transition structures to produce the two regioisomeric six-membered ring products were located, as well as ones for the 1,3-sigmatropic shifts and to form the eight-membered ring product (Figure S4 (Supporting Information)). Only the lowest energy transition state is shown in Figure 2 (**29b**, 3.9 kcal/mol barrier). This corresponds to [4 + 2] addition across the C=C double bond via the exo transition structure to give the dimer **2b**. A transition structure for an intramolecular 1, 3 proton transfer (see Figure S4 (Supporting Information), structure *ZE*-**38**-X-TS, 38.6 kcal/mol above **2b**) to give a more stable tautomer **22b** was found. This transition structure is planar and pseudopericyclic,[2d,h,3n,4c,17]

(17) Pseudopericyclic reactions lack cyclic orbital overlap and have at least four characteristics. 1. All are allowed. 2. They have nonaromatic transition states. 3. Thus, they may have very low barriers. 4. They may have planar transition states. (a) Birney, D. M.; Wagenseller, P. E. *J. Am. Chem. Soc.* **1994**, *116*, 6262−6270. (b) Birney, D. M. *J. Org. Chem.* **1994**, *59*, 2557−2564. (c) Birney, D. M. *J. Org. Chem.* **1996**, *61*, 243−251. (d) Birney, D. M.; Xu, X.; Ham, S. *Angew. Chem., Int. Ed.* **1999**, *38*, 189−193. (e) Birney, D. M. *J. Am. Chem. Soc.* **2000**, *122*, 10917−10925. (f) Fabian, W. M. F.; Barkulev, V. A.; Kappe, C. O. *J. Org. Chem.* **1998**, *63*, 5801. (g) Fabian, W. M. F.; Kappe, C. O.; Barkulev, V. A. *J. Org. Chem.* **2000**, *65*, 47−53. (h) Alajarin, M.; Vidal, A.; Sanchez-Andrada, P.; Tovar, F.; Ochoa, G. *Org. Lett.* **2000**, *2*, 965−968. (i) Alajarín, M.; Sánchez-Andrada, P.; Cossío, F. P.; Arrieta, A.; Lecea, B. *J. Org. Chem.* **2001**, *66*, 8470−8477. (j) de Lera, A. R.; Cossío, F. P. *Angew. Chem., Int. Ed.* **2002**, *41*, 1150−1152. (k) Kimball, D. B.; Herges, R.; Haley, M. M. *J. Am. Chem. Soc.* **2002**, *124*, 1572−1573.

(18) (a) Toma, L.; Romano, S.; Quadrelli, P.; Caramella, P. *Tetrahedron Lett.* **2001**, *42*, 5077−5080. (b) Caramella, P.; Quadrelli, P.; Toma, L. *J. Am. Chem. Soc.* **2002**, *124*, 1130−1131. (c) Reyes, M. B.; Lobkovsky, E. B.; Carpenter, B. K. *J. Am. Chem. Soc.* **2002**, *124*, 641−651. (d) Zhou, C.; Birney, D. M. *Org. Lett.* **2002**, *4*, 3279−3282. (e) Quadrelli, P.; Romano, S.; Toma, L.; Caramella, P. *J. Org. Chem.* **2003**, *68*, 6034−6038.

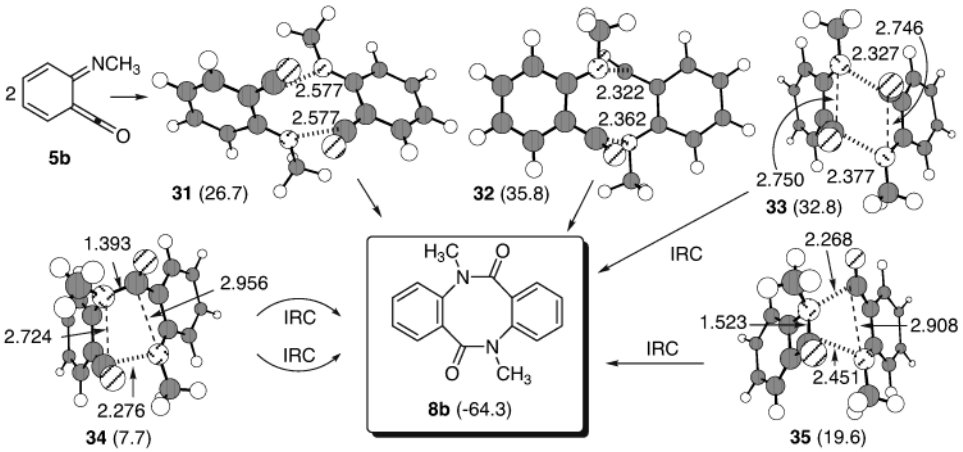

FIGURE 3. B3LYP/6-31G(d)-optimized transition structures for dimerization of **5b** and **14b** to form the eight-membered ring product **8b**. See Figure 1 for key.

but the geometry for hydrogen transfer is poor, contributing to the barrier.[17c] In view of this substantial barrier, an intermolecular pathway for this tautomerization is more likely.

Not unexpectedly, we could not locate a transition structure similar to **25a**. This may be attributed to the *N*-methyl substituent of **1b**, specifically leading to steric crowding and a lack of hydrogen bonding. These calculations are consistent with Maujean's[5a] results (eq 4) and with our experimental results in Scheme 3 that N-substitution (e.g., **1d**) leads to dimerization across the C═C bond of the ketene (e.g., **22a**) while NH-imidoylketenes (e.g., **1c**) give the regioisomeric dimers across the C═O bond (e.g., **24b**, Scheme 3).

Dimerization of *N*-Methylbenzoimidoylketene 5b. As we have shown above, **8b** can be formed under conditions where the only reactive species are N-substituted benzoimidoylketenes **5b** and the more stable ring-closed isomer **14b**.[6d,e,f] This eight-membered ring compound is formally a [4 + 4] dimer of **5b**. To explore the mechanism for the formation of **8b**, the first issue we have to address is the equilibrium between *N*-methylbenzoazetinone (**14b**) and *N*-methylbenzoimidoylketene (**5b**). The ring-closed isomer **14b** is calculated to be more stable than **5b** by 13.0 kcal/mol. The energy barrier for the ring opening of **5b** to **14b** is only 6.8 kcal/mol (see Figure S5 and Table S3 (Supporting Information), structure **38b**-TS). Thus under the conditions of the reaction, **5b** is a high energy but accessible intermediate. As found for the parent system,[4a,16] the transition structure for ring opening is planar and pseudopericyclic.[17]

There are several conceivable ways to obtain the eight-membered ring product **8b** from **14b** and **5b** including homo- and heterodimerization (Scheme 4) via either concerted or stepwise pathways. These questions were explored computationally, and the results are summarized in Figures 3 and S6 (Supporting Information), and in Tables 3 and S3 (Supporting Information).

We located five transition structures that lead to the formation of **8b** (**31**−**35**, Figure 3). In itself, this is a remarkable number of transitions states that all lead to the same product. The lowest energy transition structure for the direct [4 + 4] cycloaddition of **5b** is **31**, with a barrier of only 0.7 kcal/mol! This structure has C_2 symmetry, and is structurally very similar to the [4 + 4] transition structures for dimerization of **1a** and **1b** (**30** and structure *ZZ*-**30b**-N-TS, Figures 1 and S4-a (Supporting Information)). The primary orbital interaction seems to be donation from the nitrogen lone pairs into the in-plane ketene π^* in a pseudopericyclic manner; this likely contributes to the almost nonexistent barrier.[17] Additionally, the geometry is favorable and the reaction from two **5b** molecules to **8b** is 90.3 kcal/mol exothermic as it restores aromaticity to two rings. Nevertheless, this transition structure is 26.7 kcal/mol above two ring-closed isomers **14b** and is not the lowest energy pathway for the formation of **8b**.

Two other [4 + 4] transition structures were also found (**32** and **33**). These resemble $4\pi + 4\pi$ cycloadditions, and thus exo and endo geometries are possible. But even in these structures, the geometries suggest there is some pseudopericyclic participation of the nitrogen lone pairs. These have higher barrier, (35.8 and 32.8 kcal/mol respectively), presumably reflecting the forbidden $4\pi s + 4\pi s$ nature. A fourth transition structure (**34**) was located. While this has a low barrier of only 7.7 kcal/mol it has one of the bonds already formed. It is reminiscent of the 1,3-sigmatropic shift found above (**27a**), but following the IRC in either direction led to **8b**. We do not pretend to understand how this can be or the significance of this structure.

The lowest barrier pathway for formation of **8b** proceeds via an interesting transition state (**35**). At first glance, this looks like a transition state for ring opening of **14b** in the presence of another molecule of **5b**, but the IRC leads smoothly to **8b**.[19] This transition structure is only 19.6 kcal/mol above two **14b**. There is evidently some bonding between the two fragments, as evidenced by pyramidalization of the benzoazetinone C and N. This pathway has the lowest overall barrier because the energetic cost of ring opening the second benzoazetinone

(19) The IRC from **35** in the opposite direction from **8b** leads to a structure (Figure S6 (Supporting Information)) with one very low imaginary frequency (10.0i cm^{-1}) that corresponds not to lengthening the forming bonds, but folding the fragments together. This structure is in essence a complex between **5b** and **14b**, only 1.5 kcal/mol above a minimum energy structure. Formally, since the IRC connects two transition states, there is a valley-ridge inflection point[18] that was approximately located (Figure S6 (Supporting Information)).

14b is in part compensated for by bond formation between the fragments in **35**. Related structures on the pathway from two molecules of **14b** are presented in the Supporting Information (Figure S6 and Table S3 (Supporting Information)).

Conclusions

We have developed a novel, mild method for generation of imidoylketenes **1** from readily accessible precursors, enamino esters **9**. We have also shown that pyrolysis of **13b** leads to the [4 + 4] dimer **8b**, presumably via **14b** and **5b**. These methods have allowed us to observe a wide range of modes for the dimerization of imidoylketenes and also point to the potential for the utilization of imidoylketenes in a broader range of synthetically useful reactions.

For the N−H imidoylketenes (e.g., **5a** and **1c**), only [4 + 2] dimerization products are observed experimentally, whether under solution or flash vacuum pyrolysis conditions. In both cases, the ketene C═O is the two-atom component. The calculations on **1a** indicate that this transition structure (**25a**) is planar and pseudopericyclic and additionally is stabilized by hydrogen bonding between N_5H_{11} and N_{10}. The final step in the reaction is a nearly barrierless 1,5-prototropic shift to give the observed product (e.g., **24a**).

For N-substituted imidoylketenes, the [4 + 2] dimerization cannot be stabilized by this hydrogen bond. Instead, the observed product involves addition across the ketene C═C bond instead of the C═O bond as above. For example, **22a** arises from dimerization of **1d** and subsequent tautomerization of **2d**. This change in regiochemistry is consistent with the calculated barrier of only 3.9 kcal/mol for the lowest energy, pseudopericyclic transition structure **29b**.

For the N-substituted benzoazetinone **14b**, in equilibrium with the less stable benzoimidoylketene **5b**, an overall [4 + 4] cycloaddition is observed. A total of five different transition structures leading to the eight-memberered ring product **8b** were located. Three of these are true [4 + 4] cyclodimerizations of **5b** and the relatively low barriers are because the reactions are, at least to some degree, pseudopericyclic. But the lowest overall barrier is via sequential ring opening of one molecule of **14b** and followed by ring opening of the second **14b** in concert with dimerization via transition structure **35**.

Experimental Section

Flash Vacuum Pyrolysis of 9c. Commercially available ethyl 3-amino-2-butenoate (2.3778 g, 18.4 mmol, **9c**) was placed in a 25 mL flask connected to the FVP apparatus. The flask was cooled with liquid nitrogen, the apparatus was evacuated to approximately 0.25 Torr, and the oven was heated to 400 °C. The cooling was removed and **9c** passed through the oven over 6 h. The crude products were dissolved in 4:1 CH_2Cl_2 and Et_2O. The solution was concentrated and separated using flash chromatography on a silica gel column (6:4 hexanes/ethyl acetate). This gave 0.1029 g of the dimer **24b** (6.7%). (The assignment of the structure as **24b** instead of the tautomer **3c** is based primarily on the calculated stabilities. The hydrogen-bonded (*Z*) isomer of **24b** is preferred because the two NH hydrogens have such different chemical shifts.) Elemental analysis of the undissolved solid (**23**, 1.1008 g) suggested it was a low molecular weight polymer of **1c**, with some replacement of NH by O.

Anal. Calcd for $(C_4H_5NO)_n$: C, 57.82; H, 6.07; N, 16.86. Found: C, 55.88; H, 5.59; N, 11.14. One possible oligmer is

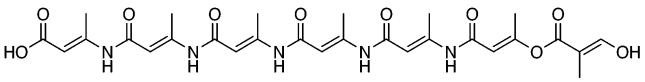

with C, 55.90; H, 5.86; N, 11.64;

24b: ^{1}H NMR (500 MHz, $CDCl_3$) δ 2.05 (s, 3H), 2.15 (d, J = 0.5 Hz, 3H), 4.75 (s, 1H), 5.15 (bs, 1H), 5.60 (d, J = 0.5 Hz, 1H), 9.11 (bs, 1H); ^{13}C NMR (125 MHz, $CDCl_3$) δ 23.1, 23.7, 85.2, 99.7, 160.4, 160.6, 165.9, 166.6; MS spectra M^+ 166, calcd for $C_8H_{10}N_2O_2^+$ 166.18; mp 108−118 °C dec, that appeared to be polymerization.

***tert*-Butyl 3-Propylamino-2-butenoate (9a).** Propylamine (0.8 mL, 9.7 mmol) was added dropwise to a 5 mL conical vial with 2 g of 4 Å molecular sieves and *tert*-butyl acetoacetate (1.6 mL, 9.6 mmol) under N_2. The solution was stirred at rt for 18 h, filtered, and washed with dry CH_2Cl_2. The solvent was evaporated, and a light yellow liquid, **9a** (1.877 g, 98.2%), was obtained:[5j] ^{1}HNMR ($CDCl_3$, 500 MHz) δ 0.95 (t, J = 7.5 Hz, 3H), 1.45 (s, 9H), 1.58 (m, 2H), 1.87 (s, 3H), 3.13 (td, J = 7.5, 6.0 Hz, 2H), 4.36 (s, 1H), 8.48 (s, 1H).

Solution Pyrolysis of 9a. Method a. *tert*-Butyl 3-propylamino-2-butenoate (0.8116 g, 4 mmol, **9a**) was added to a 5 mL conical vial with a stir bar, a Hickman still, and a condenser under N_2 atmosphere. The reaction system was heated in a 140−150 °C oil bath for 31 h. The solution was separated using flash chromatography on a silica gel column (acetone as the eluent). Product **21a** was obtained as a white solid after recrystallization from acetone (0.1272 g, 23.5%); **22a** was obtained as a white solid (0.1527 g, 30.3%, mp 52−52 °C, the stereochemistry around the exocyclic enamine bond is not confirmed), and unreacted **9a** was recovered (0.1390 g, 17.1%). From the crude NMR, the percent yields are **21a** (28.8%), **22a** (30.6%), and **9a** (40.6%).

Method b. In a 140−150 °C oil bath, *tert*-butyl 3-propylamino-2-butenoate (6.811 g, 0.034mol, **9a**) was heated in a 10 mL sealed thick-walled tube for 31 h. (**Caution**: there is a danger of explosion when heating a closed system. This reaction was conducted behind a blast shield.) The products were separated by passing through silica gel column using acetone as eluent, affording **21a** (1.0286 g, 22.7%), **22a** (0.6246 g, 14.6%), and **9a** (1.3398, 19.7%). From the crude NMR, the percent yields are **21a** (29.6%), **22a** (15.5%), and **9a** (54.9%).

21a: ^{1}H NMR (500 MHz, $CDCl_3$) δ 1.00 (t, J = 7.25 Hz, 3H), 1.56 (s, 9H), 1.63−1.71 (m, 2H), 2.30 (d, J = 0.5 Hz, 3H), 2.33 (s, 3H), 3.72−3.75 (m, 2H), 6.21 (s, 1H); ^{13}C NMR (125 MHz, $CDCl_3$) δ 10.9, 17.2, 20.5, 23.4, 28.1, 49.3, 82.1, 119.4, 126.7, 145.0, 147.9, 166.7, 174.8; IR ($CDCl_3$) ν 1632, 1720; mp 139−142 °C; MS M^+ 265, calcd for $C_{15}H_{23}NO_3^+$ 265.35. Anal. Calcd: C, 67.90; H, 8.74; N, 5.28. Found: C, 67.85; H, 9.11; N, 5.34.

22a: ^{1}H NMR (500 MHz, $CDCl_3$) δ 0.95 (t, J = 7.5 Hz, 3H), 1.04 (t, J = 7.5 Hz, 3H), 1.61−1.67 (m, 2H), 1.71−1.76 (m, 2H), 2.23 (s, 3H), 2.69 (s, 3H), 3.42 (q, J = 6.3 Hz, 2H), 3.76 (t, J = 8.0 Hz, 2H), 5.63 (s, 1H); ^{13}C NMR (125 MHz, $CDCl_3$) δ 11.3, 11.5, 18.3, 20.6, 22.4, 22.5, 45.0, 45.6, 102.7, 108.0, 148.1, 164.8, 175.8, 182.2; MS M^+ 250, calcd for $C_{14}H_{22}N_2O_2^+$ 250.17.

Solution Pyrolysis of 9c. This was carried out following method A, as described above for **9a**. A 1.388 g (10.8 mmol) portion of **9c** was heated at 150 °C for 32 h. Polymer **23** was the major product obtained (0.7655 g). In addition, 0.0132 g (1.2%) of **21b** was isolated, in analogy to **21a**: ^{1}H NMR (500 MHz, $CDCl_3$) δ 1.37 (t, J = 7.0 Hz, 3H), 2.29 (d, J = 1.0 Hz, 3H), 2.46 (s, 3H), 4.34 (q, J = 7.0 Hz, 2H), 6.26 (s, 1H), 12.05 (br s, 1H); ^{13}C NMR (125 MHz, $CDCl_3$) δ 14.47, 19.17, 21.95, 61.37, 113.35, 117.47, 147.44, 152.51, 164.36, 166.87.

Solution Pyrolysis of 13b. *N*-Methylisatoic anhydride (**13b**, 0.3501 g, 1.98 mmol) was refluxed in 1 mL of mesitylene

for 60 h with slow liberation of CO_2. The solvent was washed out using pentanes. The solid residue contains unreacted **13b** and the product **8b**. From the crude NMR, the percent yield of **8b** is 43.7%. The separation of the crude product by silica gel chromatography (10:1 chloroform/acetonitrile) gave 0.1092 g (41.5%) of **8b**.

8b: ^{1}H NMR (500 MHz, CD_3CN) δ 3.35 (s, 6H), 7.20−7.24 (m, 6H), 7.31−7.34 (m, 2H); ^{13}C NMR (125 MHz, CD_3CN) δ 36.7, 126.4, 128.3, 129.0, 131.5, 135.7, 141.4, 168.6; MS M^+ 266, calcd for $C_{16}H_{14}N_2O_2^+$ 266.29. Anal. Calcd: C, 72.16; H, 5.30; N, 10.52. Found: C, 71.94; H, 5.66, N, 10.42.

Acknowledgment. We thank Professor Thomas Tidwell for helpful discussions, the Robert A. Welch Foundation for support of this work, the Texas Tech University High Performance Computing Center for computer time, and NSF grant CHE-9808436 for the 500 MHz NMR spectrometer.

Supporting Information Available: Copies of ^{1}H and ^{13}C NMR spectra of **8b**, **21a**, **22a**, and **24b**, figures of all optimized structures, tables of absolute energies, zero-point energies and low or imaginary frequencies for all optimized structures, and IRC calculations. Cartesian coordinates of all optimized structures are available from the authors by request. This material is available free of charge via the Internet at http://pubs.acs.org.

JO035128O